of the National Center for Small Angle Scattering Research (NCSASR) at Oak Ridge provided direction and guidance in carrying out the scattering experiments. Linda Maddox of NCSASR provided the code for the ELLIPSE method of analyzing stretched specimens. The National Science Foundation supported the research with Grand DMR-8217460.

Registry No. (BDSA)(S) (copolymer), 115464-50-1; neutron, 12586-31-1.

References and Notes

(1) Kuhn, W. *Kolloid-Z.* **1936**, *76*, 258.
(2) Treloar, L. R. G. *Trans. Faraday Soc.* **1943**, *39*, 36.
(3) James, H. M.; Guth, E. *J. Chem. Phys.* **1947**, *15*, 651.
(4) James, H. M.; Guth, E. *J. Chem. Phys.* **1947**, *15*, 669.
(5) Flory, P. J. *Proc. R. Soc. London, A* **1976**, *A351*, 351.
(6) Deam, R. T.; Edwards, S. F. *Philos. Trans. R. Soc. London, A* **1976**, *A280*, 1296.
(7) Flory, P. J. *J. Chem. Phys.* **1977**, *66*, 5720.
(8) Erman, B.; Flory, P. J. *Macromolecules* **1982**, *15*, 806.
(9) Erman, B. *Macromolecules* **1987**, *20*, 1917.
(10) Bastide, J.; Picot, C.; Candau, S. J. *J. Macromol. Sci., Phys.* **1981**, *B19*, 13.
(11) Bastide, J.; Herz, J.; Boue, F. *J. Phys. (Les Ulis, Fr.)* **1985**, *46*, 1967.
(12) Ullman, R. *Macromolecules* **1982**, *15*, 582.
(13) Ullman, R. In *Elastomers and Rubber Elasticity*; Mark, J. E., Lal, J., Eds.; ACS Symposium Series 193; American Chemical Society: Washington, DC, 1982; Chapter 14.
(14) Beltzung, M.; Herz, J.; Picot, C. *Macromolecules* **1983**, *16*, 580.
(15) Williams, C.; Nierlich, M.; Cotton, J. P.; Jannink, G.; Boue, F.; Daoud, M.; Farnoux, B.; Picot, C.; de Gennes, P. G.; Rinaudo, M.; Mohan, M.; Wolff, C. *J. Polym. Sci., Polym. Lett. Ed.* **1979**, *17*, 370.
(16) Akcasu, A. Z.; Summerfield, G. C.; Jahshan, S. N.; Han, C. C.; Kim, C. Y.; Yu, H. *J. Polym. Sci., Polym. Phys. Ed.* **1980**, *18*, 863.
(17) Benoit, H.; Koberstein, J.; Leibler, L. *Makromol. Chem., Suppl.* **1981**, *4*, 85.
(18) Ullman, R. *J. Chem. Phys.* **1979**, *71*, 436.
(19) Ullman, R. *Macromolecules* **1982**, *15*, 1395.
(20) Edwards, S. F. *Proc. Phys. Soc., London* **1966**, *88*, 265.
(21) Dermer, O. C.; Edmison, M. T. *J. Am. Chem. Soc.* **1955**, *77*, 70.
(22) Heacock, J. F.; Edmison, M. T. *J. Am. Chem. Soc.* **1960**, *82*, 3460.
(23) Abramovitch, R. A.; Knaus, G. N.; Uma, V. *J. Org. Chem.* **1974**, *8*, 1101.
(24) Breslow, D. S.; Sloan, M. F.; Newburg, N. R.; Renfrow, W. B. *J. Am. Chem. Soc.* **1969**, *91*, 2273.
(25) Charlesby, A. *Proc. R. Soc. London, A* **1954**, *A222*, 542.
(26) Ullman, R. *J. Polym. Sci., Polym. Lett. Ed.* **1983**, *21*, 521.
(27) Ullman, R. *J. Polym. Sci., Polym. Phys. Ed.* **1984**, *23*, 1477.
(28) Summerfield, G. C.; Mildner, D. F. R. *J. Appl. Crystallogr.* **1983**, *16*, 384.
(29) Reynolds, L. E.; Mildner, D. F. R. *J. Appl. Crystallogr.* **1984**, *17*, 411.
(30) Wignall, G. D.; Bates, F. S. *J. Appl. Crystallogr.* **1987**, *20*, 28.
(31) King, J. S.; Boyer, W.; Wignall, G. D.; Ullman, R. *Macromolecules* **1985**, *18*, 709.
(32) Bauer, D. R.; Ullman, R. *Macromolecules* **1980**, *13*, 709.
(33) Strazielle, C.; Benoit, H. *Macromolecules* **1975**, *8*, 203.
(34) Daoud, M.; Cotton, J. P.; Farnoux, B.; Jannink, G.; Sarma, G.; Benoit, H.; Duplessix, R.; Picot, C.; de Gennes, P. G. *Macromolecules* **1975**, *8*, 704.
(35) Wiltzius, P.; Haller, H. R.; Cannell, D. S.; Schaefer, D. W. *Phys. Rev. Lett.* **1983**, *51*, 1183.
(36) Rawiso, M.; Duplessix, R.; Picot, C. *Macromolecules* **1987**, *20*, 630.
(37) O'Reilly, J. M.; Teegarden, D. M.; Wignall, G. D. *Macromolecules* **1985**, *18*, 2747.
(38) Benoit, H.; Decker, D.; Duplessix, R.; Picot, C.; Rempp, P.; Cotton, J. P.; Farnoux, B.; Jannink, G.; Ober, R. *J. Polym. Sci., Polym. Phys. Ed.* **1976**, *14*, 2119.
(39) Davidson, N. S.; Richards, R. W. *Macromolecules* **1986**, *19*, 2576.
(40) Soni, V.; Stein, R. S., private communication. Soni, V. Ph.D. Dissertation, University of Massachusetts, 1986.

Equilibrium Morphology of Block Copolymer Melts. 2

Kyozi Kawasaki, Takao Ohta,* and Mitsuharu Kohrogui

Department of Physics, Faculty of Science, Kyushu University 33, Fukuoka 812, Japan.
Received October 8, 1987

ABSTRACT: Our earlier theory on the same subject (Ohta, T.; Kawasaki, K. *Macromolecules*, **1986**, *19*, 2621) was reformulated so as to exhibit the scaling behavior inherent in the free energy functional. In this way we naturally recover the domain size of mesophases behaving as the two-thirds power of the polymerization index. The higher order long-range interactions of the parameter field are found not to be small and indicate a need to accurately calculate free energies in various mesophases, which is a purely geometrical problem in the strong segregation limit of the symmetric block copolymer model.

1. Introduction

In the previous paper to be referred to as part 1 on the same subject[1] we developed a theory of equilibrium morphology of block copolymer melts on the basis of Leibler's field-theoretic formulation.[2] There we have shown that effects of connectedness of the two blocks can be represented by repulsive (attractive) Coulomb-type forces between the monomers of the same (different) species. Here the main approximation for the model was that the part of the free-energy functional containing the long-range interaction of the local monomer concentration fluctuation can be represented by the above-mentioned Coulomb-type two-body interactions where we have seen cancellation of leading terms of the higher order interactions of long range. However, effects of the terms left out are yet to be examined. Indeed we will find that these terms are by no means negligible.

Another significant result which was found but was not stressed in part 1 is that in the strong segregation limit the dimensionless relative free energies of various mesophases are functions of the volume fraction of the A-rich domains uniquely determined by the geometry of the mesophase structures. Thus it is interesting to see how general this result is beyond the specific approximation made in part 1.

Under this circumstance we here reformulate the problem of equilibrium morphology of a block copolymer melt. Although we start in section 2 with the field-theoretic formalism as in part 1 and in Leibler's work, we do not rely on the mean-field approximation from the outset to derive the free-energy functional. The mean-field approximation will be replaced by certain assumptions like that associated

---

*Address correspondence to this author at the Department of Physics, Ochanomizu University, Tokyo 112, Japan.

© 1988 American Chemical Society

with incompressibility (section 3) and the Gaussian chain statistics (section 5). In section 4 we show a scaling behavior of the free energy functional, thereby demonstrating the domain size growing as a two-thirds power of the polymerization index. We also find there and in section 5 that the higher order long-range interactions emerge which were left in part 1 and scale in the same way as those retained in part 1. Attempts are made in section 7 to estimate numerically these higher order contributions.

2. Field Theory of Block Copolymers

We consider a system composed of n diblock copolymer chains, each containing N_K monomers of species K with K = A and B. We denote by $\mathbf{c}$ a configuration of the entire polymer system and by $H(\mathbf{c})$ the microscopic Hamiltonian whose precise form is not specified. The partial monomer number densities are expressed as

$$\hat{\rho}_A(\mathbf{r}) = \int_0^{N_A} d\tau \sum_{i=1}^{n} \delta(\mathbf{r} - \mathbf{c}_i(\tau)) \tag{2.1a}$$

$$\hat{\rho}_B(\mathbf{r}) = \int_{N_A}^{N} d\tau \sum_{i=1}^{n} \delta(\mathbf{r} - \mathbf{c}_i(\tau)) \tag{2.1b}$$

where each chain is parametrized by τ along its length ($0 < \tau < N = N_A + N_B$) and $\mathbf{c}_i(\tau)$ is the position vector of the monomer at τ of the i-th polymer chain. The local order parameter is then given by

$$\hat{\psi}(\mathbf{r}) = \sum_{K}^{A,B} f_K \hat{\rho}_K(\mathbf{r}) \tag{2.2}$$

with

$$f_A \equiv N_B/N = 1 - f \qquad f_B = -N_A/N = -f \tag{2.3}$$

Throughout the paper we use symbols with carets to denote microscopic expressions. We note from (2.2) and (2.3) that

$$\int \hat{\psi}(\mathbf{r})\, d\mathbf{r} = 0 \tag{2.4}$$

In the following it is most useful to employ the field-theoretic formalism of Brezin and others,[3] which has been adapted to block copolymers by Leibler.[2] However, in contrast to Leibler, at this stage we neither assume any specific form for $\hat{H}(\mathbf{c})$ nor rely on the mean-field approximation. We then introduce the field $\phi(\mathbf{r})$, which is conjugate to $\hat{\psi}(\mathbf{r})$, and also the generating functional $W\{\phi\}$ by

$$W\{\phi\} = \ln [Z\{\phi\}/Z\{0\}] \tag{2.5}$$

$$Z\{\phi\} \equiv \int d\mathbf{c} \exp\left\{-\hat{H}(\mathbf{c}) + \int d\mathbf{r}\, \phi(\mathbf{r})\, \hat{\psi}(\mathbf{r})\right\} \tag{2.6}$$

where the Boltzmann constant times the absolute temperature has been equated to unity for simplicity. Next we introduce another functional $H\{\psi\}$ as

$$H\{\psi\} = -W\{\phi\} + \int d\mathbf{r}\, \phi(\mathbf{r})\, \psi(\mathbf{r}) \tag{2.7}$$

where $\psi(\mathbf{r})$ and $\phi(\mathbf{r})$ are not independent but are related as

$$\psi(\mathbf{r}) = \delta W\{\phi\}/\delta\phi\{\mathbf{r}\} = \langle \hat{\psi}(\mathbf{r}) \rangle_{\{\phi\}} \tag{2.8}$$

The notation implies that $\psi(\mathbf{r})$ is indeed the average value of $\hat{\psi}(\mathbf{r})$ in the presence of the conjugate field $\phi(\mathbf{r})$. Naturally we can require

$$\int \psi(\mathbf{r})\, d\mathbf{r} = 0 \tag{2.4$'$}$$

Then we also find

$$\phi(\mathbf{r}) = \delta H\{\psi\}/\delta\psi(\mathbf{r}) \tag{2.9}$$

The conjugate field can play the role of a symmetry-breaking field which can be set to zero afterward, where (2.9) with $\phi(\mathbf{r}) = 0$ gives the order parameter profile in a mesophase state of block copolymers. Here we should stress generality of this approach: (1) all the fluctuation effects are included in the partition function (2.6), and (2) although we focus our attention only on the order parameter profile, other variables such as the total density are not left out of the problem.

The generating functional $W\{\phi\}$ is now expanded as

$$W\{\phi\} = \sum_{m=1}^{\infty} \frac{1}{m!} C_m(\bar{1}\ \bar{2} \ldots \bar{m}) \phi(\bar{1})\ \phi(\bar{2}) \ldots \phi(\bar{m}) \tag{2.10}$$

where we have introduced the shorthand notations: j stands for $\mathbf{r}_j$ and upper bars indicate integrations. Then we have

$$\begin{aligned} C_m(1\ 2 \ldots m) &= [\delta^m W\{\phi\}/\delta\phi(1)\ \delta\phi(2) \ldots \delta\phi(m)]_{\{\phi\}=0} \\ &= \langle \hat{\psi}(1)\ \hat{\psi}(2) \ldots \hat{\psi}(m) \rangle_c \end{aligned} \tag{2.11}$$

where the angular bracket denotes a connected average.

Likewise $H\{\psi\}$ is expanded as

$$H\{\psi\} = \sum_{m=2}^{\infty} \frac{1}{m!} \Gamma_m(\bar{1}\ \bar{2} \ldots \bar{m}) \psi(\bar{1})\ \psi(\bar{2}) \ldots \psi(\bar{m}) \tag{2.12}$$

Absence of the term $m = 1$ in (2.12) is due to the fact that

$$\Gamma_1(\mathbf{r}) = [\delta H\{\psi\}/\delta\psi(\mathbf{r})]_{\{\psi\}=0} = [\phi(\mathbf{r})]_{\{\psi\}=0} \tag{2.13}$$

should generally vanish. We again have

$$\Gamma_m(1\ 2 \ldots m) = [\delta^m H\{\psi\}/\delta\psi(1)\ \delta\psi(2) \ldots \delta\psi(m)]_{\{\psi\}=0} \tag{2.14}$$

The Γ's are readily expressed in terms of the C's if we substitute (2.9) into the right-hand side (rhs) of (2.7) and compare the coefficients of expansion of the both sides in powers of the ψ's. Here we list the first three such expressions:

$$\Gamma_2(1\ 2) = C_2^{-1}(1\ 2) \tag{2.15a}$$

$$\Gamma_3(1\ 2\ 3) = -C_2^{-1}(1\ \bar{1})\ C_2^{-1}(2\ \bar{2})\ C_3^{-1}(3\ \bar{3})\ C_3(\bar{1}\ \bar{2}\ \bar{3}) \tag{2.15b}$$

$$\begin{aligned} \Gamma_4(1\ 2\ 3\ 4) = {} & C_2^{-1}(1\ \bar{1})\ C_2^{-1}(2\ \bar{2})\ C_2^{-1}(3\ \bar{3})\ C_2^{-1}(4\ \bar{4}) \\ & \{-C_4(\bar{1}\ \bar{2}\ \bar{3}\ \bar{4}) + C_2^{-1}(\bar{5}\ \bar{6})[C_3(\bar{1}\ \bar{2}\ \bar{5})\ C_3(\bar{3}\ \bar{4}\ \bar{6}) + {} \\ & C_3(\bar{1}\ \bar{3}\ \bar{5})\ C_3(\bar{2}\ \bar{4}\ \bar{6}) + C_3(\bar{1}\ \bar{4}\ \bar{5})\ C_3(\bar{2}\ \bar{3}\ \bar{6})]\} \end{aligned} \tag{2.15c}$$

where C_2^{-1} is the inverse function defined by

$$C_2^{-1}(1\ \bar{2})\ C_2(\bar{2}\ 3) = \delta(1\ 3) \tag{2.16}$$

$\delta(ij)$ being the delta function $\delta(\mathbf{r}_i - \mathbf{r}_j)$.

Since we have translational invariance for $\phi(\mathbf{r}) = \psi(\mathbf{r}) = 0$, it is sometimes more convenient to consider Fourier transforms $\tilde{C}$ and $\tilde{\Gamma}$ of the C's and the Γ's, respectively, defined for $m \geq 2$ as

$$\tilde{C}_m(\mathbf{q}_1 \ldots \mathbf{q}_m) = V^{-1} \int d\mathbf{r}_1 \ldots \int d\mathbf{r}_m\ C_m(\mathbf{r}_1 \ldots \mathbf{r}_m) \times \exp(i\mathbf{q}_1 \cdot \mathbf{r}_1 + \ldots + i\mathbf{q}_m \cdot \mathbf{r}_m) \tag{2.17}$$

and similarly for $\tilde{\Gamma}_m$, where V is the system volume.

So far everything is formal and exact and does not even reflect in any substantial way the fact that we are dealing with polymers. To make further progress we need to know the properties of the Γ's and hence the C's.

3. Strong Segregation Limit

In this paper we will be exclusively concerned with the strong segregation limit in which there is a strong repulsive interaction between monomers of different species. This can be represented by the local free energy density of the form

$$-\tfrac{1}{2} \int d\mathbf{r}\ \chi \hat{\psi}^2(\mathbf{r}) \tag{3.1}$$

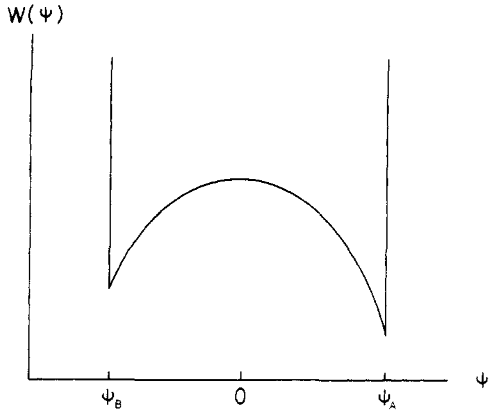

Figure 1. Local free energy function.

where χ is the positive Flory–Huggins interaction parameter.[4]

We also assume the system to be incompressible. This condition is expressed by saying that the total local average monomer density $\rho(\mathbf{r}) = \rho_A(\mathbf{r}) + \rho_B(\mathbf{r})$ is uniquely determined by the local relative concentration of the two species:

$$\rho(\mathbf{r}) = F[\psi(\mathbf{r})/\rho(\mathbf{r})] \tag{3.2}$$

Now, ψ/ρ is restricted to be in the interval between $f_B < 0$ and $f_A > 0$, and, hence, for a smooth function F, the values of ρ are also limited in some interval, say, between $\rho_{\min}$ and $\rho_{\max}$. Expressing (3.2) in terms of $\psi(\mathbf{r})$ as a function of $\rho(\mathbf{r})$, which is assumed to be nonsingular, we see that the values of $\psi(\mathbf{r})$ are restricted to be in some interval, say, between $\psi_B < 0$ and $\psi_A > 0$. In particular, if F is a constant so that $\rho(\mathbf{r}) = \rho_0$(constant), we find $\psi_A = \rho_0 N_A/N$ and $\psi_B = -\rho_0 N_B/N$. But this restriction is not necessary. We can write (3.2) as

$$\psi = xF(x) \qquad x = \psi/\rho \tag{3.2$'$}$$

Since x is bounded by f_B and f_A, the bounds on ψ to be denoted as ψ_B and ψ_A are given by the minimum and maximum, respectively, of $xF(x)$ for x between f_B and f_A. The corresponding total densities are denoted as ρ_{0B} and ρ_{0A}, which can be different from each other. As we shall see below, in order for the strongly segregated states with domains consisting of pure A or B type monomers to be realized, the extrema of $xF(x)$ should occur at the two bounds of x, namely, f_B and f_A, which will be assumed to be the case hereafter. Otherwise, strong segregation will be hindered by the incompressibility effects. Thus we can take

$$\psi_A = f_A\rho_{0A} \qquad \psi_B = f_B\rho_{0B} \tag{3.3}$$

With the above consideration we see that the local free energy density W expressed as a function of $\psi(\mathbf{r})$ consists of the two terms

$$W(\psi) = w_0(\psi) - \tfrac{1}{2}\chi\psi^2 \tag{3.4}$$

in which $\hat{\psi}$ in (3.1) has been replaced by ψ, neglecting effects of local fluctuations of $\hat{\psi}$. $W_0(\psi)$ is a smooth function in the interval (ψ_B,ψ_A) and is infinite outside. See Figure 1.

As χ tends to very large values in the strong segregation limit, two very sharp minima start to appear in $W(\psi)$ at $\psi = \psi_A$ and ψ_B. Then we will have well-defined domains with ψ equal either to ψ_A or to ψ_B. Note that in contrast to two-phase states of usual phase separation, the two minima of $W(\psi)$ need not be equal. A block copolymer system is still a one-component system in the thermodynamic sense and the volume fraction ϕ_A of the domain with $\psi = \psi_A$ is fixed by the condition (2.4) or by

$$\phi_A = -\psi_B/(\psi_A - \psi_B) = \frac{(1 - f_A)\rho_{0B}}{\rho_{0B} + f_A(\rho_{0A} - \rho_{0B})} \tag{3.5}$$

Since the two components of each block copolymer chain cannot be separated, we have mesophases with sharp domain walls.

The properties of the local free energy described above *must be derivable from the microscopic free energy* $\hat{H}(\mathbf{c})$ and thus should be reflected in the actual form of $H\{\psi\}$, (2.12). The task of actually verifying this is, however, formidable and will not be attempted. Here we merely try to identify the terms in $H\{\psi\}$ responsible for such mesophase structures.

First we divide without loss of generality the functions $\tilde{\Gamma}_m\{\mathbf{q}\}$, the Fourier transform of $\Gamma_m(1\ 2\ ...\ m)$, into two parts as

$$\tilde{\Gamma}_m\{\mathbf{q}\} = \tilde{\Gamma}_m{}^{S}\{\mathbf{q}\} + \tilde{\Gamma}_m{}^{L}\{\mathbf{q}\} \tag{3.6}$$

where $\tilde{\Gamma}_m{}^{S}\{\mathbf{q}\}$ remains finite as all the $\mathbf{q}$ variables tend to zero whereas $\tilde{\Gamma}_m{}^{L}\{\mathbf{q}\}$ vanishes when all the $|\mathbf{q}|$ tend to infinity. Here we associate the terms which vanish as all the $|\mathbf{q}|$ diverge but remain finite for vanishing $|\mathbf{q}|$ with $\tilde{\Gamma}_m{}^{S}\{\mathbf{q}\}$. Then $\tilde{\Gamma}_m{}^{L}\{\mathbf{q}\}$ diverges as all the $|\mathbf{q}|$ tend to zero. Next we make a plausible assumption that $\tilde{\Gamma}_m{}^{S}\{\mathbf{q}\}$ can be expanded in an ascending series of the $\mathbf{q}$'s so that the corresponding function $\Gamma_m{}^{S}(1, 2, ..., m)$ has a cluster property. That is, $\Gamma_m{}^{S}(1, 2, ..., m)$ practically vanishes whenever any pair of the points 1, 2, ..., m is separated by a distance greater than some finite length, say, r_0, much smaller than $N^{1/2}b$, b being the segment length. We argue that $H^S\{\psi\}$ which is $H\{\psi\}$ where all the Γ's are replaced by Γ^S's describes phase-separated states with well-defined domains. That is, the associated Euler equation which minimizes $H^S\{\psi\}$ under the condition (3.4)

$$\sum_{m=1}^{\infty} \frac{1}{m!}\Gamma_{m+1}{}^{S}(\mathbf{r}, \bar{1}\ \bar{2}\ ...\ \bar{m})\ \psi(\bar{1})\ \psi(\bar{2})\ ...\ \psi(\bar{m}) = \lambda \tag{3.7}$$

λ being the Lagrange multiplier arising from (2.4), should have solutions of the following two types: (i) uniform states with constant $\psi(\mathbf{r})$ equal either to ψ_A or to ψ_B; (ii) states with a flat domain wall which divides two domains with $\psi = \psi_A$ and $\psi = \psi_B$. The domain wall thickness ξ is of the order of $r_0/\chi^{1/2}$ and is much smaller than other length scales such as the dimension of a chain.[5]

The domain wall encountered here is something like a domain wall in a ferromagnet under an external field, which is not stationary and moves in the direction of decreasing the magnetic free energy. Here such a domain wall is made stationary by the constraint (2.4).

Since the volume fraction of one of the domains, ϕ_A, cannot be changed, the only relevant part of $H^S\{\psi\}$ is the domain wall free energy. Thus we have, omitting an unimportant constant part,

$$H^S\{\psi\} = \sigma A \tag{3.8}$$

where σ is the domain wall free energy per unit wall area and A is the total domain wall area in the system.

$H^S\{\psi\}$ alone, however, is inadequate, of course, to describe mesophase morphology or the equilibrium domain structures, and we now focus on the remainder denoted as $H^L\{\psi\}$:

$$H^L\{\psi\} = \sum_{m=2}^{\infty} \frac{1}{m!}\Gamma_m{}^{L}(\bar{1}\ \bar{2}\ ...\ \bar{m})\ \psi(\bar{1})\ \psi(\bar{2})\ ...\ \psi(\bar{m}) = V\sum_{m=2}^{\infty} \frac{1}{m!}\int_{\mathbf{q}_1} ... \int_{\mathbf{q}_m} \tilde{\Gamma}_m{}^{L}(\mathbf{q}_1, \mathbf{q}_2, ..., \mathbf{q}_m)\tilde{\psi}_{\mathbf{q}_1}\tilde{\psi}_{\mathbf{q}_2} ... \tilde{\psi}_{\mathbf{q}_m} \tag{3.9}$$

where

$$\int_{\mathbf{q}} \equiv \frac{1}{V}\sum_{\mathbf{q}} = \frac{1}{(2\pi)^3}\int \mathrm{d}\mathbf{q} \tag{3.10}$$

and

$$\tilde{\psi}_{\mathbf{q}} \equiv \int e^{-i\mathbf{q}\cdot\mathbf{r}}\psi(\mathbf{r})\ \mathrm{d}\mathbf{r} \tag{3.11}$$

Here $\psi(\mathbf{r})$ can be taken to represent some well-defined domain structures.

Let us now assume that the Γ^{L}'s or the $\tilde{\Gamma}^{\mathrm{L}}$'s are dominated by long-range order parameter correlations which are partially justified by the results obtained below. Then polymer chain statistics can be used to study the behavior of these functions.

One surprising fact about polymer melts is that equilibrium statistics of long-chain molecule obeys the Gaussian law. This law, which is also referred to as Flory's theorem,[4] is considered to be asymptotically exact for large polymerization indices. We should also note that the repulsive interactions between monomers of different species have already been taken into account in $H^{\mathrm{S}}\{\psi\}$. We hence assume the Gaussian statistics of ideal polymer chains. Then there exists a characteristic length, the gyration radius of a chain, which is simply denoted as $N^{1/2}$, omitting a prefactor with the dimension of length. (We will not worry about dimensions of various quantities.) Then, in view of the definitions (2.1), (2.2), and (2.11), $\tilde{C}_{\mathrm{m}}$ with $m \geq 2$, which correspond to ideal Gaussian chains, should have a prefactor $V^{-1}nN^m = \rho_0 N^{m-1}$ where ρ_0 is the total monomer density since

$$\tilde{\psi}_{\mathbf{q}} \equiv \int e^{-i\mathbf{q}\cdot\mathbf{r}}\hat{\psi}(\mathbf{r})\ \mathrm{d}\mathbf{r} = \int_0^N \mathrm{d}\tau\ f(\tau)\sum_{i=1}^{n}\exp(-i\mathbf{q}\cdot\mathbf{C}_i(\tau)) \tag{3.12}$$

contributes a factor N from each chain and different chains are statistically independent in the Gaussian case. Here we have defined

$$\begin{aligned} f(\tau) &= f_{\mathrm{A}} \qquad 0 < \tau < N_{\mathrm{A}} \\ &= f_{\mathrm{B}} \qquad N_{\mathrm{A}} < \tau < N \end{aligned} \tag{3.13}$$

so that we have

$$\int_0^N f(\tau)\ \mathrm{d}\tau = 0 \tag{3.14}$$

which is another expression of the property (2.4).

Therefore we can write, denoting the set $\mathbf{q}_1, ..., \mathbf{q}_m$ simply as $\{\mathbf{q}\}$

$$\tilde{C}_m\{\mathbf{q}\} = N^{m-1}e_m\{N^{1/2}\mathbf{q}\} \qquad (m \geq 2) \tag{3.15}$$

where e_m is a scaling function which can also depend on f_{K}.

Using relations like (2.15) or their Fourier transforms, we also find the following scaling behavior:

$$\tilde{\Gamma}_m{}^{\mathrm{L}}\{\mathbf{q}\} = N^{-1}\gamma_m\{N^{1/2}\mathbf{q}\} \tag{3.16}$$

the scaling function γ_m again depending also on f_{K}.

The foregoing analysis is now summarized in the following form for $H\{\psi\}$:

$$H\{\psi\} = \sigma A + V\sum_{m=2}^{\infty}\frac{1}{m!}\int_{\mathbf{q}_1}\cdots\int_{\mathbf{q}_m}N^{-1}\gamma_m\{N^{1/2}\mathbf{q}\}\tilde{\psi}_{\mathbf{q}_1}\tilde{\psi}_{\mathbf{q}_2}\cdots\tilde{\psi}_{\mathbf{q}_m} \tag{3.17}$$

where by definition γ_m should tend to zero for all $\{\mathbf{q}\}$ much greater than $N^{-1/2}$.

We end this section by a remark on possible asymmetry effects of the two species on Gaussian averages following the discussion of Helfand and Sapse.[6] Here it is useful to recall arbitrariness of the choice of a monomer unit. Thus the values of N_{A} and N_{B} as well as the Kuhn length b_{A} and b_{B} can depend on this arbitrariness. However, the combinations $N_{\mathrm{A}}b_{\mathrm{A}}{}^2$ as well as $N_{\mathrm{B}}b_{\mathrm{B}}{}^2$ are no longer arbitrary since they are the square of the gyration radii of the A and B blocks of a block copolymer, respectively. Thus, we can incorporate asymmetry effects of the two species in the following discussions by reinterpreting N_{K} to mean $N_{\mathrm{K}}b_{\mathrm{K}}{}^2$. We further assume absence of volume change of mixing of monomers of the two species so that the total system volume can be fixed.

4. Scaling Behavior

In strongly segregated diblock copolymer, the A–B junctions of polymer chains lie on domain walls. This has the effects of extending polymers chain in the perpendicular direction to the domain wall beyond the gyration radius $N^{1/2}$. This extension will characterize the scale of mesophase domain structure, which is denoted as l and will greatly exceed the gyration radius. Then $\tilde{\psi}_{\mathbf{q}}$ will be important mainly for $|\mathbf{q}| \sim l^{-1}$ where $|N^{1/2}\mathbf{q}|$ are very small. To see this in more detail, we have to study the small $|\mathbf{q}|$ behavior of the $\tilde{\Gamma}^{\mathrm{L}}$'s for which we also need the small $|\mathbf{q}|$ behavior of the $\tilde{C}$'s by relations like (2.15). For this purpose we make use of the multipole expansion of $\hat{\psi}(\mathbf{r})$ to be described now.

We start from (3.12) which we rewrite by using the position vector $\bar{\mathbf{c}}_i$ of the i-th chain defined as

$$\bar{\mathbf{c}}_i \equiv \frac{1}{N}\int_0^N \mathrm{d}\tau\ \mathbf{c}_i(\tau) \tag{4.1}$$

Thus we have

$$\tilde{\psi}_{\mathbf{q}} = \sum_i e^{-i\mathbf{q}\cdot\bar{\mathbf{c}}_i}\int_0^N f(\tau)e^{-i\mathbf{q}\cdot\delta\mathbf{c}_i(\tau)}\ \mathrm{d}\tau \tag{4.2}$$

with

$$\delta\mathbf{c}_i(\tau) \equiv \mathbf{c}_i(\tau) - \bar{\mathbf{c}}_i \tag{4.3}$$

Expanding the integrand of (4.2) we have using (3.14)

$$\tilde{\psi}_{\mathbf{q}} = \sum_i e^{-i\mathbf{q}\cdot\bar{\mathbf{c}}_i}\left[-i\mathbf{q}\cdot\hat{\mathbf{P}}_i - \frac{1}{2}\mathbf{q}\mathbf{q}:\hat{\mathbf{Q}}_i + ...\right] \tag{4.4}$$

where the expansion coefficients are multipole moment tensors of the i-th chain given by

$$\hat{\mathbf{P}}_i \equiv \int_0^N \delta\mathbf{c}_i(\tau)\ f(\tau)\ \mathrm{d}\tau \tag{4.5a}$$

$$\hat{\mathbf{Q}}_i \equiv \int_0^N \delta\mathbf{c}_i(\tau)\ \delta\mathbf{c}_i(\tau)\ \mathrm{f}(\tau)\ \mathrm{d}\tau \qquad \text{etc.} \tag{4.5b}$$

The corresponding expression for $\hat{\psi}(\mathbf{r})$ is

$$\hat{\psi}(\mathbf{r}) = -\nabla\cdot\hat{\mathbf{P}}(\mathbf{r}) + {}^1\!/\!_2\nabla\nabla:\hat{\mathbf{Q}}(\mathbf{r}) \tag{4.6}$$

where the multipole moment tensor densities are given by

$$\hat{\mathbf{P}}(\mathbf{r}) \equiv \sum_i \hat{\mathbf{P}}_i\delta(\mathbf{r} - \bar{\mathbf{c}}_i) \tag{4.7a}$$

$$\hat{\mathbf{Q}}(\mathbf{r}) \equiv \sum_i \hat{\mathbf{Q}}_i\delta(\mathbf{r} - \bar{\mathbf{c}}_i) \qquad \text{etc.} \tag{4.7b}$$

In order to evaluate the connected Gaussian averages $\tilde{C}_m$ it is enough to consider the single-chain contributions and multiply the results by n in view of the statistical independence of different ideal Gaussian chains. Thus, (4.4) can be temporarily replaced by

$$\hat{\psi}_{\mathbf{q}} = -i\mathbf{q}\cdot\hat{\mathbf{P}} - {}^1\!/\!_2\mathbf{q}\mathbf{q}:\hat{\mathbf{Q}} + ... \tag{4.8}$$

where the suffices i and the factor $\exp(-i\mathbf{q}\cdot\bar{\mathbf{c}}_i)$ have been omitted due to translational invariance. By definition, connected Gaussian averages of $\hat{\mathbf{P}}$ which is linear in $\hat{\mathbf{c}}(\tau)$ disappear. Hence nonvanishing connected Gaussian averages necessarily involve higher moments. Thus we consider a connected Gaussian average of the following form appearing in C_m:

$$\langle X_1 X_2 \ldots X_m \rangle_c \tag{4.9}$$

where X_i is a multipole moment containing p_j factors of $\mathbf{c}(\tau)$. This connected average can be represented graphically by wires. Since at least $m-1$ wires are required, we must have

$$\sum_{j=1}^{m} p_j \geq 2(m-1) \tag{4.10}$$

Since each factor of $\mathbf{c}(\tau)$ carries with it a wave vector collectively denoted as $\mathbf{q}$, (4.9) should behave for small $\mathbf{q}$ at most as

$$\langle X_1 X_2 \ldots X_m \rangle_c \sim q^{2(m-1)} \tag{4.11}$$

Hence $\tilde{C}_m\{\mathbf{q}\}$ for the n-chain system should behave in the same way. This fact is combined with (3.15) to obtain

$$\tilde{C}_m\{\mathbf{q}\} = N^{2(m-1)} q^{2(m-1)} \tilde{e}_m\{N^{1/2}\mathbf{q}\}, \qquad m \geq 2 \tag{4.12}$$

where, barring accidental cancellation,

$$\tilde{e}_{\mathrm{m}}\{\mathbf{0}\} = \text{finite} \tag{4.13}$$

From the relationships like (2.15) we then find

$$\tilde{\Gamma}_m{}^{\mathrm{L}}\{\mathbf{q}\} = \rho_0{}^{3m-5} N^{-2} q^{-2} \tilde{\gamma}_m\{N^{1/2}\mathbf{q}\} \tag{4.14}$$

where

$$\lim_{\mathbf{q}_i \to 0} \tilde{\gamma}_m\{N^{1/2}\mathbf{q}\} = \text{finite} \tag{4.15}$$

and we have extracted powers of some length l_0 so that the $\tilde{\gamma}$'s become dimensionless quantities. By construction, $\tilde{\gamma}_m\{N^{1/2}\mathbf{q}\}$ must be such that (4.14) should vanish when all the $|\mathbf{q}|$'s go to infinity. If this were not the case the nonvanishing part must have been associated with $\tilde{\Gamma}_m{}^{\mathrm{S}}\{\mathbf{q}\}$ as mentioned before. This ambiguous situation, however, does not affect the small $|\mathbf{q}|$ behavior of (4.14) with the $\mathbf{q}$'s in $\tilde{\gamma}_m$ equated to zero.

The total free energy functional density per unit volume now takes the following form:

$$V^{-1}H\{\psi\} = \sigma(A/V) + \sum_{m=2}^{\infty} \frac{1}{m!} \int_{\mathbf{q}_1} \cdots \int_{\mathbf{q}_m} N^{-2} \bar{q}_m{}^{-2} \tilde{\gamma}_m\{N^{1/2}\mathbf{q}\} \tilde{\psi}_{\mathbf{q}_1} \tilde{\psi}_{\mathbf{q}_2} \ldots \tilde{\psi}_{\mathbf{q}_m} \tag{4.16}$$

where $\bar{q}_m$ is a typical size of the $\mathbf{q}$'s like $[\sum_i^m \mathbf{q}_i{}^2/m]^{1/2}$. Now, what we have said about the behavior of $\psi_{\mathbf{q}}$ at the beginning of this section suggests the following changes of variables:

$$\tilde{\psi}_{\mathbf{q}} = (l/l_0)^3 \bar{\psi}_{\mathbf{k}} \qquad \mathbf{k} = l\mathbf{q} \tag{4.17}$$

where l is some length to be determined. Then A/V, which has the dimension of inverse length, is scaled as

$$A/V = l^{-1}\bar{A} \tag{4.18}$$

where $\bar{A}$ is the dimensionless domain wall area density. Then (4.16) reduces with $\bar{k}_m \equiv l\bar{q}_m$ to

$$V^{-1}H\{\psi\} = \frac{\sigma}{l}\bar{A} + l_0{}^{-5} N^{-2} l^2 \sum_{m=2}^{\infty} \frac{1}{m!} \int_{\mathbf{k}_1} \cdots \int_{\mathbf{k}_m} \bar{k}_m{}^{-2} \tilde{\gamma}_m\{(N^{1/2}/l)\mathbf{k}\} \bar{\psi}_{\mathbf{k}_1} \bar{\psi}_{\mathbf{k}_2} \ldots \bar{\psi}_{\mathbf{k}_m} \tag{4.19}$$

We can now choose l to be

$$l = (\sigma l_0{}^5)^{1/3} N^{2/3} \tag{4.20}$$

Since $N^{1/2}/l$ behaves as $N^{-1/6}$ and the k's are of the order of unity, the arguments in the $\tilde{\gamma}$'s can be replaced by zero provided the integrals in (4.19) converge at large $|\mathbf{k}|$. We assume this to be the case, which will be discussed later. Then we have

$$V^{-1}H\{\psi\} = \frac{\sigma}{l} h\{\bar{\psi}\} \tag{4.21}$$

with $h\{\psi\}$ the dimensionless free energy density given by

$$h\{\bar{\psi}\} = \bar{A} + \sum_{m=2}^{\infty} \frac{1}{m!} \int_{\mathbf{k}_1} \cdots \int_{\mathbf{k}_m} g_m(\omega_m)\ \bar{k}_m{}^{-2} \bar{\psi}_{\mathbf{k}_1} \bar{\psi}_{\mathbf{k}_2} \ldots \bar{\psi}_{\mathbf{k}_m} \tag{4.22}$$

where $g_m(\omega_m)$ is given by (4.15) which can depend on the relative orientations ω_m of $\mathbf{k}_1, \mathbf{k}_2, \ldots, \mathbf{k}_m$.

Note that all the quantities appearing in (4.22) are dimensionless, and the length l, (4.20), gives the linear dimension of mesophase domains as a function of the polymerization index, which reproduces the result of references 1, 2, 5, and 6. Now, $\bar{\psi}_{\mathbf{k}}$ represents a Fourier transform of the domain structure function. Thus, if the wavenumber is much greater than the inverse of the average domain size but is much smaller than the domain wall thickness, $\bar{\psi}_{\mathbf{k}}$ would behave as k^{-3} in three dimensions because of rapid cancellations inside domains. The integrand in (4.22) thus goes like k^{-3m-2} and the integral is ultraviolet convergent. (This result is compatible with the Porod law $\langle|\bar{\psi}_{\mathbf{k}}|^2\rangle \propto k^{-4}$ for random domain wall systems.[7] For instance, for even m the Porod law contribution to (4.22) arising from pairwise factorizations of the ψ's behaves as $k_0{}^{-m/2-2}$ with k_0 ($>N^{-1/2}$) the lower wavenumber cutoff, which is smaller than $k_0{}^{-2}$, which we have here.) We should note in passing that the factor N^{-2} in front of the second term of (4.19) implies its weakness in the sense that perturbations from this term are not strong enough to disrupt the sharp domain wall states but only act to influence the equilibrium domain wall configurations.

For subsequent discussion it is convenient to choose l_0 such that

$$l_0{}^3(\psi_{\mathrm{A}} - \psi_{\mathrm{B}}) = l_0{}^3(f_{\mathrm{A}}\rho_{0\mathrm{A}} - f_{\mathrm{B}}\rho_{0\mathrm{B}}) = 1 \tag{4.23}$$

Then, the dimensionless local order parameter $\bar{\psi}(l^{-1}\mathbf{r}) \equiv l^3\psi(\mathbf{r})$, which is also the inverse Fourier transform of $\bar{\psi}_{\mathbf{k}}$, takes on the two values $\bar{\psi}_{\mathrm{A}}$ and $\bar{\psi}_{\mathrm{B}}$ in the A-rich and the B-rich domains, respectively, which are determined by the two conditions (4.23) and (2.4). Namely,

$$\bar{\psi}_{\mathrm{A}} - \bar{\psi}_{\mathrm{B}} = 1 \qquad \bar{\psi}_{\mathrm{A}}\phi_{\mathrm{A}} + \bar{\psi}_{\mathrm{B}}(1 - \phi_{\mathrm{A}}) = 0 \tag{4.24}$$

That is,

$$\bar{\psi}_{\mathrm{A}} = 1 - \phi_{\mathrm{A}} \qquad \bar{\psi}_{\mathrm{B}} = -\phi_{\mathrm{A}} \tag{4.25}$$

Now, the dimensionless free energy is seen to have certain universal aspects. $g_m(\omega_m)$ depends, besides ω_m, only on the ratio f. Under a change of length scale by a factor, say, υ, which results from changing the choice of l, (4.20), the two terms of (4.22) are multiplied by υ^{-1} and υ^2, respectively. Then, for given values of f and ϕ_{A}, we can minimize (4.22) to obtain an equilibrium morphology of the two domains. This minimization basically results from balancing of the two terms of (4.22). Under this length scale change, the length scale of morphology measured in l is naturally increased by the factor υ. The minimized free energy, however, remains the same. Thus as far as determination of equilibrium morphology of domains is concerned, no adjustable parameter remains once the overall length scale is fixed. Namely, the equilibrium mesophase domain structure is uniquely determined by the two physically observable parameters $f = N_{\mathrm{A}}b_{\mathrm{A}}{}^2/$

$(N_Ab_A^2 + N_Bb_B^2)$ and $\phi_A = N_A\rho_{0B}/(N_B\rho_{0A} + N_A\rho_{0B})$. Note that as is expected ϕ_A is invariant under the changes $N_k \rightarrow b_k^2N_k$ and $\rho_{0k} \rightarrow b_k^2\rho_{0k}$. Furthermore, if we also require the symmetry of the two species such that $b_A^2\rho_{0A} = b_B^2\rho_{0B}$, then we have only a single parameter $\phi_A = f$. Analogous situation arises also if only the $m = 2$ term is retained in the rhs of (4.22), since g, which is a constant, can be absorbed by a change of the length scale, as indeed was the case in paper 1. Thus, for the two last-mentioned special cases, the problem becomes purely geometrical and the equilibrium morphology (aside from overall length scale) is uniquely determined by the volume fraction of one of the species.

5. Long-Range Contributions

Here we obtain expressions of the first few $\tilde{\Gamma}^L$ functions for small wavenumbers. For this we also need the C functions, which can be also written as

$$\tilde{C}_m\{\mathbf{q}\} = (n/V)\tilde{C}^*{}_m\{\mathbf{q}\} \tag{5.1}$$

with

$$\tilde{C}^*{}_m\{\mathbf{q}\} \equiv \langle\tilde{\psi}_{\mathbf{q}_1}\tilde{\psi}_{\mathbf{q}_2}\ \dots\ \tilde{\psi}_{\mathbf{q}_3}\rangle_c \tag{5.2}$$

where (5.2) is computed for a single polymer chain.

Then we find

$$\tilde{\Gamma}_m\{\mathbf{q}\} = (n/V)^{1-m}\tilde{\Gamma}^*{}_m\{\mathbf{q}\} \tag{5.3}$$

where $\tilde{\Gamma}^*{}_m\{\mathbf{q}\}$ is obtained for a single polymer chain. In this section all the connected averages are for a single chain with the following microscopic Hamiltonian:

$$\tilde{H}_G(\mathbf{c}) = \frac{1}{2}\int_0^N \mathrm{d}\tau \left[\frac{\mathrm{d}\mathbf{c}(\tau)}{\mathrm{d}\tau}\right]^2 = \frac{1}{N}\sum_{p=0}^{\infty}\left(\frac{\pi p}{N}\right)^2 \tilde{\mathbf{c}}_p^{\,2} \tag{5.4}$$

Here $\mathbf{c}(\tau)$ was expanded in terms of normal modes $\tilde{\mathbf{c}}_p$ with free end as

$$\mathbf{c}(\tau) = \frac{2}{N}\sum_{p=0}^{N}\tilde{\mathbf{c}}_p \cos\frac{\pi p}{N}\tau \tag{5.5}$$

Hence we have, denoting the unit dyadic by $\mathbf{1}$,

$$\langle\tilde{\mathbf{c}}_p\tilde{\mathbf{c}}_{p'}\rangle = \delta_{pp'}\mathbf{1}\frac{N}{2}\left(\frac{N}{\pi p}\right)^2 \tag{5.6}$$

The multipole moments are then expressed as

$$\mathbf{P} = \frac{2}{N}{\sum_p}'\tilde{f}_p\tilde{\mathbf{c}}_p \tag{5.7}$$

$$\mathbf{Q} = \frac{1}{2}{\sum_p}'{\sum_{p'}}'\left(\frac{2}{N}\right)^2[\tilde{f}_{p+p'} + \tilde{f}_{p-p'}]\tilde{\mathbf{c}}_p\tilde{\mathbf{c}}_{p'} \qquad \text{etc.} \tag{5.8}$$

where

$$\tilde{f}_p \equiv \int_0^N f(\tau)\cos\frac{\pi p}{N}\tau\ \mathrm{d}\tau = \frac{N}{\pi p}\sin \pi f p \tag{5.9}$$

and primes on summation signs exclude the $p = 0$ terms. First we take up $\tilde{\Gamma}_2^L(\mathbf{q})$. For small $|\mathbf{q}|$ we find (5.6) and (5.7)

$$\tilde{C}^*{}_2(q) = q^2\langle P_x^{\,2}\rangle_c = T_2q^2 \tag{5.9$'$}$$

with

$$T_2 \equiv \frac{2}{N}{\sum_p}'\left(\frac{N}{\pi p}\right)^4 \sin^2 \pi p f \tag{5.10}$$

Next we consider $\tilde{C}^*{}_3\{\mathbf{q}\}$, which is the sum of the terms of the form $\langle\mathbf{QPP}\rangle_c$. After some algebra we find

$$\tilde{C}^*{}_3(\mathbf{q}_1\mathbf{q}_2\mathbf{q}_3) = T_3[(\mathbf{q}_1\cdot\mathbf{q}_2)(\mathbf{q}_1\cdot\mathbf{q}_3) + (\mathbf{q}_2\cdot\mathbf{q}_3)(\mathbf{q}_2\cdot\mathbf{q}_1) + (\mathbf{q}_3\cdot\mathbf{q}_1)(\mathbf{q}_3\cdot\mathbf{q}_2)] \tag{5.11}$$

with $\mathbf{q}_1 + \mathbf{q}_2 + \mathbf{q}_3 = 0$ and

$$T_3 \equiv \frac{2}{N^2}{\sum_p}'{\sum_{p'}}'\left(\frac{N}{\pi p}\right)^2\left(\frac{N}{\pi p'}\right)^2[\tilde{f}_{p+p'} + \tilde{f}_{p-p'}]\tilde{f}_p\tilde{f}_{p'} \tag{5.12}$$

$\tilde{C}^*{}_4\{\mathbf{q}\}$ consists of two types of terms of the forms $\langle\mathbf{QQPP}\rangle_c$ and $\langle\mathbf{UPPP}\rangle_c$ with $\mathbf{U}$ is the octapole moment. The result is, with $\mathbf{q}_1 + \mathbf{q}_2 + \mathbf{q}_3 + \mathbf{q}_4 = 0$,

$$\tilde{C}^*{}_4(\mathbf{q}_1\mathbf{q}_2\mathbf{q}_3\mathbf{q}_4) = -T_4^{\,Q}\overset{(6)}{\sum}(\mathbf{q}_1\cdot\mathbf{q}_2)[(\mathbf{q}_1\cdot\mathbf{q}_3)(\mathbf{q}_2\cdot\mathbf{q}_4) + (\mathbf{q}_1\cdot\mathbf{q}_4)(\mathbf{q}_2\cdot\mathbf{q}_3)] - T_4^{\,U}\overset{(4)}{\sum}(\mathbf{q}_1\cdot\mathbf{q}_2)(\mathbf{q}_1\cdot\mathbf{q}_3)(\mathbf{q}_1\cdot\mathbf{q}_4) \tag{5.13}$$

where $\sum^{(6)}$ and $\sum^{(4)}$ are the summations over six and four terms, respectively, obtained by interchanging indices for symmetrizing the results. The coefficients $T_4^{\,Q}$ and $T_4^{\,U}$ which correspond to the two terms arising from $\langle\mathbf{QQPP}\rangle_c$ and $\langle\mathbf{UPPP}\rangle_c$, respectively, are given by

$$T_4^{\,Q} \equiv \frac{2}{N^3}{\sum_p}'{\sum_{p'}}'{\sum_{p''}}'(\tilde{f}_{p+p'} + \tilde{f}_{p-p'}) \times (\tilde{f}_{p'+p''} + \tilde{f}_{p'-p''})\tilde{f}_p\tilde{f}_{p''}\left(\frac{N}{\pi p}\right)^2\left(\frac{N}{\pi p'}\right)^2\left(\frac{N}{\pi p''}\right)^2 \tag{5.14a}$$

$$T_4^{\,U} \equiv \frac{2}{N^3}{\sum_p}'{\sum_{p'}}'{\sum_{p''}}'(\tilde{f}_{p+p'+p''} + \tilde{f}_{p-p'+p''} + \tilde{f}_{p+p'-p''} + \tilde{f}_{p-p'-p''})\tilde{f}_p\tilde{f}_{p'}\tilde{f}_{p''}\left(\frac{N}{\pi p}\right)^2\left(\frac{N}{\pi p'}\right)^2\left(\frac{N}{\pi p''}\right)^2 \tag{5.14b}$$

With these results we are now ready to write down the first few $\tilde{\Gamma}^*$'s using (2.15)

$$\tilde{\Gamma}^*{}_2(\mathbf{q}) = T_2^{-1}q^{-2} \tag{5.15a}$$

$$\tilde{\Gamma}^*{}_3(\mathbf{q}_1,\mathbf{q}_2,\mathbf{q}_3) = -T_2^{-3}T_3q_1^{-2}q_2^{-2}q_3^{-2}[(\mathbf{q}_1\cdot\mathbf{q}_2)(\mathbf{q}_1\cdot\mathbf{q}_3) + (\mathbf{q}_2\cdot\mathbf{q}_3)(\mathbf{q}_2\cdot\mathbf{q}_1) + (\mathbf{q}_3\cdot\mathbf{q}_1)(\mathbf{q}_3\cdot\mathbf{q}_2)] \tag{5.15b}$$

$$\begin{aligned}\tilde{\Gamma}^*{}_4(\mathbf{q}_1\mathbf{q}_2\mathbf{q}_3\mathbf{q}_4) = {} & T_2^{-4}\mathbf{q}_1^{-2}\mathbf{q}_2^{-2}\mathbf{q}_3^{-2}\mathbf{q}_4^{-2}\{T_4^{\,Q}\overset{(6)}{\sum}(\mathbf{q}_1\cdot\mathbf{q}_2)[(\mathbf{q}_1\cdot\mathbf{q}_3)\cdot(\mathbf{q}_2\cdot\mathbf{q}_4) + (\mathbf{q}_1\cdot\mathbf{q}_4)(\mathbf{q}_2\cdot\mathbf{q}_3)] + T_4^{\,U}\overset{(4)}{\sum}(\mathbf{q}_1\cdot\mathbf{q}_2)(\mathbf{q}_1\cdot\mathbf{q}_3)(\mathbf{q}_1\cdot\mathbf{q}_4) + {} \\ & T_2^{-1}T_3^{\,2}\overset{(3)}{\sum}[(\mathbf{q}_1\cdot\mathbf{q}_2)(\mathbf{q}_1\cdot\mathbf{q}_5) + (\mathbf{q}_1\cdot\mathbf{q}_2)(\mathbf{q}_2\cdot\mathbf{q}_5) + (\mathbf{q}_1\cdot\mathbf{q}_5)(\mathbf{q}_2\cdot\mathbf{q}_5)]\mathbf{q}_5^{-2} \times \\ & [(\mathbf{q}_3\cdot\mathbf{q}_4)(\mathbf{q}_3\cdot\mathbf{q}_5) + (\mathbf{q}_3\cdot\mathbf{q}_4)(\mathbf{q}_4\cdot\mathbf{q}_5) - (\mathbf{q}_3\cdot\mathbf{q}_5)(\mathbf{q}_4\cdot\mathbf{q}_5)]\}\end{aligned} \tag{5.15c}$$

where the sum of the $\mathbf{q}$'s in each $\tilde{\Gamma}^*{}_m$ has been chosen to be zero and in (5.15c) we have put $\mathbf{q}_5 = -\mathbf{q}_1 - \mathbf{q}_2 = \mathbf{q}_3 + \mathbf{q}_4$. The summations in (5.15) are over proper combinations of the $\mathbf{q}$'s to symmetrize the $\tilde{\Gamma}^*{}_m$'s in the wave vectors and the number of the terms in the various summations are shown in parentheses.

T_m generally behaves as

$$T_m = N^{2m-1}t_m(f) \tag{5.16}$$

which, together with (5.1), conforms to the general results (4.12) and hence (4.14).

6. Equilibrium Free Energy

Here we attempt to evaluate the equilibrium free energy for the ordered structures. As was done in ref 1, 2, 5, and 6 we consider three structures. One is a lamellar structure alternating the A-rich domains and B-rich domains. The width of the A-rich domains is denoted by R. Two other structures are a triangular lattice of disks and a bcc structure of spheres with radius R of the A-rich domains.

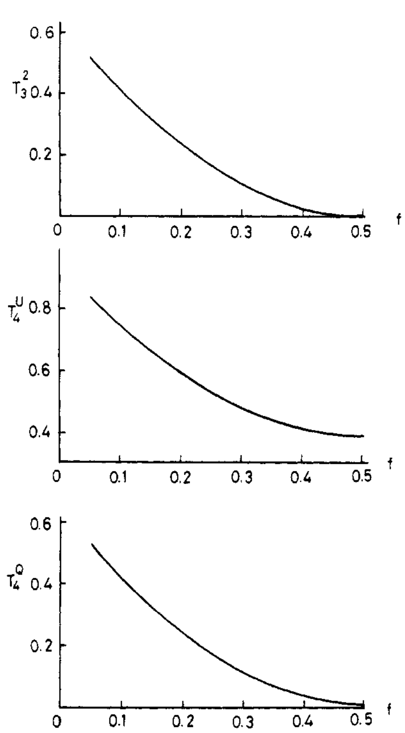

Figure 2. Plots of T_3^2, T_4^U, and T_4^Q versus f.

We do not distinguish the volume fraction $\phi = \phi_A$ of the A-rich domains and the block ratio f since these two quantities are identical with each other in the extremely strong segregation limit of the symmetrical case $\rho_{0A} = \rho_{0B}$ in (3.5) to be considered here.

The long-range part of the free energy functional is given from (3.9), (5.3), and (5.15) by

$$H^{L}\{\psi\} \equiv \sum_{m=2}^{\infty} H_m{}^{L}\{\psi\} = \left(\frac{3\rho_0}{N}\right)\left(\frac{a^2}{N}\right) \times \sum_{m=2}^{\infty} \frac{1}{m!}\left(\frac{1}{f(1-f)}\right)^m f^m \sum_{\mathbf{k}_1\ldots\mathbf{k}_m}{}' \delta_{\sum_i \mathbf{k}_i,0}\hat{\Gamma}^{(m)}(\mathbf{k}_1 \ldots \mathbf{k}_m) \times \bar{\psi}\left(\mathbf{k}_1\frac{R}{a}\right) \ldots \bar{\psi}\left(\mathbf{k}_m\frac{R}{a}\right) \quad (6.1)$$

where $\hat{\Gamma}^{(m)}$ are given up to $m = 4$ by

$$\hat{\Gamma}^{(2)}(\mathbf{k}_1,\mathbf{k}_2) = 1/k_1{}^2 \quad (6.2)$$

$$\hat{\Gamma}^{(3)}(\mathbf{k}_1,\mathbf{k}_2,\mathbf{k}_3) = -\hat{T}_3(f)\frac{k_1{}^2k_2{}^2 - (\mathbf{k}_1\cdot\mathbf{k}_2)^2}{k_1{}^2k_2{}^2k_3{}^2} \quad (6.3)$$

$$\hat{\Gamma}^{(4)}(\mathbf{k}_1,\mathbf{k}_2,\mathbf{k}_3,\mathbf{k}_4) = 12\hat{T}_4{}^Q(f)\frac{(\mathbf{k}_1\cdot\mathbf{k}_2)(\mathbf{k}_1\cdot\mathbf{k}_3)(\mathbf{k}_2\cdot\mathbf{k}_4)}{k_1{}^2k_2{}^2k_3{}^2k_4{}^2} + 4\hat{T}_4{}^U(f)\frac{(\mathbf{k}_1\cdot\mathbf{k}_2)(\mathbf{k}_1\cdot\mathbf{k}_3)(\mathbf{k}_1\cdot\mathbf{k}_4)}{k_1{}^2k_2{}^2k_3{}^2k_4{}^2} - 3\hat{T}_3(f)^2\frac{(k_1{}^2k_2{}^2 - (\mathbf{k}_1\cdot\mathbf{k}_2)^2)(k_3{}^2k_4{}^2 - (\mathbf{k}_3\cdot\mathbf{k}_4)^2)}{k_1{}^2k_2{}^2k_3{}^2k_4{}^2(\mathbf{k}_1 + \mathbf{k}_2)^2} \quad (6.4)$$

The functions $\hat{T}_3$, $\hat{T}_4{}^Q$, and $\hat{T}_4{}^U$ are now dimensionless and given respectively by

$$\hat{T}_3 = \frac{3^2}{N^3}\left(\frac{1}{f(1-f)}\right)^3 T_3 \quad (6.5)$$

$$\hat{T}_4{}^{Q,U} = \frac{3^3}{N^n}\left(\frac{1}{f(1-f)}\right)^4 T_4{}^{Q,U} \quad (6.6)$$

The T's are the decreasing functions of f as shown in Figure 2. The lattice constant of an ordered mesophase structure is denoted by a. In the strong segregation limit the ratio R/a is given by

$$\begin{aligned} R/a &= f \quad \text{(lamellar)} \\ &= (3^{1/2}f/2\pi)^{1/2} \quad \text{(disk)} \\ &= (3f/8\pi)^{1/3} \quad \text{(sphere)} \end{aligned} \quad (6.7)$$

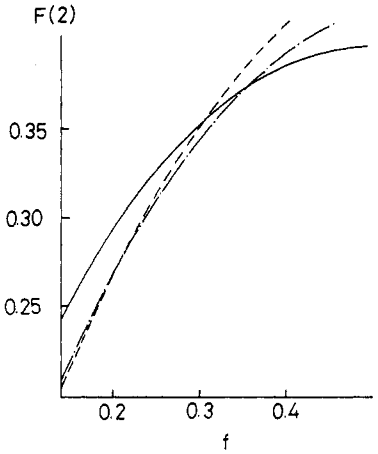

Figure 3. Second-order term of the free energy versus f for lamellar (—), cylindrical (-··-), and spherical (- - -) structures.

The function $\bar{\psi}(x)$ is the structure function of the d-dimensional hypersphere:

$$\begin{aligned} \bar{\psi}(x) &= \frac{2}{x}\sin(x/2) \quad d = 1 \\ &= \frac{2}{x}J_1(x) \quad d = 2 \\ &= \frac{3}{x^3}(\sin x - x\cos x) \quad d = 3 \end{aligned} \quad (6.8)$$

with $J_1(x)$ the Bessel function. Finally $\mathbf{k}_i$ are the reciprocal lattice vectors.

The $m = 2$ term in (6.1) was obtained in part 1 by the Ewald method. The results are summarized as follows.

$$\begin{aligned} \sum_{\mathbf{k}}{}' \frac{1}{k^2}\bar{\psi}\left(\mathbf{k}\frac{R}{a}\right)\bar{\psi}\left(\mathbf{k}\frac{R}{a}\right) &= \frac{1}{12}(1-f)^2 \quad \text{(lamellar)} \\ &= \frac{3^{1/2}}{8\pi}(-c^*{}_1 + f - \ln f) \quad \text{(disk)} \\ &= 2\left(\frac{3}{8\pi}\right)^{2/3} f^{-1/3}(0.2 + 0.1f - c^*{}_2 f^{1/3}) \quad \text{(sphere)} \end{aligned} \quad (6.9)$$

where $c^*{}_1 = 0.997\,49$ and $c^*{}_2 = 0.298\,64$. By taking into account the short-range part H^S, (3.8), in the free energy functional we thus obtain the equilibrium free energy. The results are displayed in Figure 3. Note here that the free energies of the different structures meet each other almost tangentially at f_{cl}, and especially at f_{sc}. The transition from the spherical structure (bcc) to the cylindrical structure and from the cylindrical structure to the lamellar structure occur respectively at the critical values f_{sc} and f_{cl} of f given by

$$f_{sc} = 0.194 \quad \text{and} \quad f_{cl} = 0.35 \quad (6.10)$$

These values are slightly different from those obtained in part 1 since we have used the approximation $c^*{}_1 = 1$ and $c^*{}_3 = 0.3$ there.

Here we wish to correct two transcriptional errors in part 1. The coefficient in (3.18a) should carry an extra factor $1/N$. The coefficient 1/3 in (4.43) should be replaced by $1/\xi$.

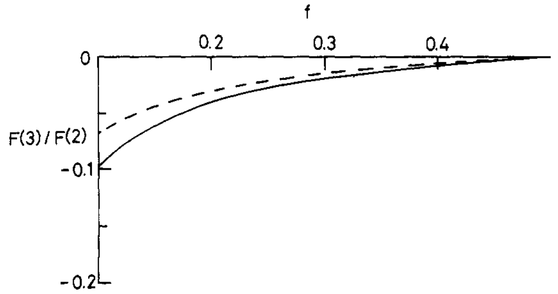

Figure 4. Ratio of the third-order term of the long-range part of the free energy H_L to the second-order term H_L versus f for cylindrical (—) and spherical (- - -) structures.

Now we examine the higher order corrections $m > 3$ in (6.1). This is, however, a very difficult task. One of the reasons is the slowness of the convergence of the summation over $\mathbf{k}_i$. We have applied the Ewald method to the lowest order term with $m = 2$. A similar method is possible in principle for the higher order terms as well. In practice, however, the resulting expressions would become terribly complicated. More serious is the fact that the expansion (6.1) does not possess any smallness parameter of the expansion. Thus we cannot evaluate the higher order corrections in a controllable manner.

This is what one should generally expect in the strong segregation limit where the reduced dimensionless amplitude of modulation is of the order of unity [see (4.25)].[9] We have attempted without success to see any general structure of higher order terms in the expansion by angular preaveraging like (6.12). Nevertheless we would like to point out the difference of our scheme from the naive expansions and truncation at finite order of $H\{\psi\}$, (2.12). We have included all the expansion terms in the short-wavelength components of $\psi(\mathbf{r})$ which contribute to the domain wall energy but have only truncated the expansion in powers of long-wavelength components of $\psi(\mathbf{r})$.

For the reasons mentioned, here at this time we can only present a rough estimation of the H_3^L term. It is readily found from (6.3) that H_3^L for a lamellar structure vanishes identically. We have calculated H_3^L numerically for a triangular lattice and a bcc lattice. The reciprocal lattice vector $\mathbf{k}$ takes the form $\mathbf{k} = (2\pi(n_1 - n_2), 2\pi(n_1 + n_2)/(3^{1/2}), 0)$, for a triangular lattice, and $\mathbf{k} = (2\pi(m_1 + m_2), 2\pi(m_2 + m_3), 2\pi(m_1 + m_3))$ for a bcc lattice where n_i and m_i are integers. We have introduced the upper cutoff for $|\mathbf{k}|$ such that $|n_i| \leq 10$ ($i = 1, 2$) and $|m_i| \leq 5$ ($i = 1, 2, 3$). The results are displayed in Figure 4. The correction H_3^L is apparently small compared to H_2^L. For instance $H_3^L/H_2^L \cong 0.1$ at $f = 0.036$. However, as can be seen from Figure 3, this correction results in a rather large shift of the critical values of f. In fact we obtain the following new critical values:

$$f_{sc} \simeq 0.29 \qquad f_{cl} \simeq 0.40 \tag{6.11}$$

Since the convergence of the summation in (6.1) is slow, the values given in (6.11) are not precise. We may say only that the critical values increase rather substantially by the correction H_3^L. We have performed an alternative estimation of H_3^L. That is, we replaced $\hat{\Gamma}^{(3)}$, (6.3), by its angular average:

$$\hat{\Gamma}^{(3)}(\mathbf{k}_1,\mathbf{k}_2,\mathbf{k}_3) \Rightarrow -\hat{T}_3(f)\frac{d-1}{d}\frac{1}{k_3^2} \tag{6.12}$$

Using the fact that $\bar{\psi}(\mathbf{r})^2 = \bar{\psi}(\mathbf{r})$ where $\bar{\psi}(\mathbf{r}) = 1$ in the A-rich domains and vanishes elsewhere we see that H_3^L is proportional to H_2^L and can be expressed by (6.9). The critical values f_{sc} and f_{cl} obtained in this way are given by

$$f_{sc} = 0.335 \qquad f_{cl} = 0.42 \tag{6.13}$$

These are not far from (6.11).

A very preliminary numerical estimation of H_4^L indicates that H_4^L is larger than H_3^L. In fact, we obtain $H_4^L/H_2^L > 1$ for a lamellar structure and $H_4^L/H_2^L > 0.5$ for a cylindrical structure both for $f > 0.35$. Thus it is impossible at present to obtain reliable estimates for the values of f_{sc} and f_{cl} including the higher order corrections.

7. Discussions

In this work we have reformulated the field-theoretical approach to the equilibrium morphology of block copolymer melts so as to retain as much generality as possible and to exhibit clearly the general scaling behavior. The results indicate existence of higher order long-range interaction terms which produce significant corrections to the threshold critical values of f for different mesophase structures in the strong segregation limit of the symmetrical model. Here all the parameters are scaled out and the calculation is "purely" geometrical. In view of the necessity of very accurate determinations of free energies for reliable estimates of these threshold values, our present estimates of the latter should not be taken too seriously. However, the results do indicate the need and importance of calculating the threshold values of f with sufficient accuracy, including higher order long-range interactions, which are now determined by geometry and are completely independent of adjustable parameters although accurate computation appears to be a rather formidable task.

The present analysis also applies to more complicated kinds of mesophase structures such as the tetrapod phase,[8] and the problem again reduces to a purely geometrical one in the strong segregation limit of the symmetrical model. The computational difficulty, however, is stupendous.

Despite all these findings we express a hope that our simple free energy functional of part 1 still serves as a useful model to represent real block copolymer systems.

Finally we would like to comment on the related work by Semenov.[10] In his work the spatial distribution of junction points plays a more important role than in ours and acts as a source charge density in the electrostatic analogue. Thus the relationship with our theory is not clear at this time. Further progress may be made if we generalize our formalism by including the junction point density field $\rho_J(\mathbf{r})$ in addition to the ψ-field. The Semenov theory should come out if we first eliminate ψ by functional integration or by minimization with $\rho_J(\mathbf{r})$ fixed. (In fact the general formalism of section 2 also applies *verbatim* when there are more than one type of fields, simply by supposing that $\psi(j)$ etc. stand for $\psi_{\alpha_j}(\mathbf{r}_j)$ etc., where α_j specifies the type of field and spatial integrations include summations over the α's as well. Such formal generalizations may well be worthwhile. For instance, in this way one can study single-chain conformation[11] by including variables like $\delta(\mathbf{r} - \mathbf{c}_1(\tau))$. As far as final results are concerned, Semenov obtains $f_{sc} = 0.12$ and $f_{cl} = 0.28$, which are quite different from our values, (6.10). The difference is not surprising since Semenov's free energy values are approximate (with an accuracy no worse than 20%) and we know from section 6 that the threshold values of f for different mesophases are very sensitive to uncertainties in the free energy evaluations.

Acknowledgment. We thank referees for constructuve criticisms which improved the manuscript. The work was supported in part by the Scientific Research Fund of the Ministry of Education, Science and Culture.

References and Notes

(1) Ohta, T.; Kawasaki, K. *Macromolecules* **1986**, *19*, 2621.
(2) Leibler, L. *Macromolecules* **1980**, *13*, 1602.

Macromolecules 1988, *21*, 2980–2987

(3) Brezin, E.; Le Guillou, J. C.; Zinn-Justin, J. In *Phase Transitions and Critical Phenomena*; Domb, C., Green, M. S., Eds.; Academic: London, 1976; Vol. 6.

(4) de Gennes, P.-G. *Scaling Concepts in Polymer Physics*; Cornell University: Ithaca, NY, 1979.

(5) Helfand, E.; Wasserman, Z. R. In *Developments in Block Copolymers*; Goodman, I., Ed.; Applied Science: London, 1982; Vol. 1.

(6) Helfand, E.; Sapse, A. M. *J. Chem. Phys.* **1975**, *62*, 1327.

(7) Porod, G. In *Small Angle X-ray Scattering*; Glatter, O., Kratky, O., Eds.; Academic: London, 1982.

(8) Hasegawa, H.; Sumitomo, T.; Hashimoto, T.; Kawai, H.; Presented at the 32nd Polymer Symposium, Society of Polymer Science, Japan, 1983; *Polym. Prepr., Jpn.* **1983**, *32*, 1695. Hasegawa, H.; Tanaka, H.; Yamasaki, K.; Hashimoto, T., *Macromolecules* **1987**, *20*, 1651. Alward, D. B.; Kinning, D. J.; Thomas, E. L.; Fetters, L. J. *Macromolecules* **1986**, *19*, 215.

(9) One can also consider a regime in which the modulation amplitude is small. However, when the polymerization index is extremely large such that the domain size becomes much greater than the domain wall thickness, the reduced amplitude again reaches the size of the order unity and then we are no longer in the weak segregation regime. In fact, the relevant dimensionless parameter that decides the degree of segregation is χN_K where χ is the Flory–Huggins interaction parameter and N_K is the smaller of N_A and N_B.[1,5,10]

(10) Semenov, A. N., *Sov. Phys.—JETP (Engl. Transl.)* **1985**, *61*(4), 733.

(11) Hasegawa, H.; Hashimoto, T.; Kawai, H.; Lodge, T. P.; Amis, E. J.; Glinka, C.; Han, C. C. *Macromolecules* **1985**, *18*, 67. Hasegawa, H.; Tanaka, H.; Hashimoto, T. *Macromolecules* **1987**, *20*, 2120.

Interfacial Tension of Immiscible Polymer Blends: Temperature and Molecular Weight Dependence

Spiros H. Anastasiadis

Polymer Materials Program, Department of Chemical Engineering, Princeton University, Princeton, New Jersey 08544

Irena Gancarz

Technical University of Wroclaw, Wroclaw, Poland

Jeffrey T. Koberstein*

Institute of Materials Science and Department of Chemical Engineering, University of Connecticut, Storrs, Connecticut 06268.

Received January 27, 1988;
Revised Manuscript Received April 26, 1988

ABSTRACT: Interfacial tensions between immiscible homopolymers are measured by using an automated pendant drop apparatus, which utilizes video digital image processing techniques. A recently developed robust shape analysis algorithm is used to analyze the experimental drop profiles. The data show the effect of temperature and number average molecular weight (M_n) on the interfacial tension for the immiscible blends polystyrene–poly(methyl methacrylate), polybutadiene–poly(dimethylsiloxane) and polystyrene–hydrogenated 1,2-polybutadiene. Interfacial tension decreases linearly with temperature and increases with molecular weight. The data are well represented by an $C_1 + C_2M_n^{-z}$ dependence on molecular weight but are not of sufficient precision to determine a precise value for the exponent. The interfacial tension data for the latter blend system are compared with thermodynamic theories of polymeric interfaces. A square gradient theory approach, in conjunction with the Flory–Huggins expression for the free energy of mixing, predicts a magnitude and temperature dependence of interfacial tension which are in reasonable agreement with experimental data. The predicted molecular weight dependence corresponds well with experimental data at high molecular weights but severely underestimates the interfacial tensions for low molecular weights.

Introduction

The structure and thermodynamic state of polymeric interfaces are important features in many polymeric materials of current technological interest. This is especially true for multiconstituent systems such as immiscible polymer blends or microphase separated copolymers, where interface structure can affect greatly the mechanical properties.[1] Interfacial tension is important due to its influence on the morphology of multiphase polymers. A number of experimental investigations, for example, have shown that the phase structure (e.g. dispersed particle size) in incompatible polymer blends is directly proportional to the interfacial tension.[2-4]

Fundamentally, interfacial tension is a thermodynamic property of the system which may be calculated directly from statistical thermodynamic theories. Experimental measurement of interfacial tensions is therefore a straightforward means for evaluating the validity of these theories.

The existent data pertaining to the interfacial properties of multiphase polymers have been well summarized in several reviews[5-7] and a monograph by Wu.[8] Interfacial tension generally decreases linearly with temperature with a temperature coefficient in the range of 10^{-2} dyn/(cm °C). An increase in molecular weight leads to an increase in the interfacial tensions; however, there are only a few studies which have examined this dependence in any detail. Experimental interfacial tensions[9,10] between *n*-alkanes and a perfluoroalkane ($C_{12.5}F_{27}$), poly(dimethylsiloxane) (PDMS) and $C_{12.5}F_{27}$ or C_8F_{18}, and alkanes with poly(ethylene glycol) all exhibit an apparent $M_n^{-2/3}$ dependence on molecular weight (where M_n is the number average molecular weight), similar to what has been found for homopolymer surface tension.[8]

This similarity is predicted by several empirical theories which relate interfacial tension to the pure component surface tensions.[11,12] A number of thermodynamic theories[13-20] have appeared that predict the interfacial tensions of polymer blends. The applicability of these theories has been discussed in detail in several review articles.[5,7,8,21,22] To date, these theories have not been compared to data

---

* To whom correspondence should be addressed.

0024-9297/88/2221-2980$01.50/0 © 1988 American Chemical Society